Epigenetic Silencing of Interferon-κ in Human Papillomavirus Type 16–Positive Cells

Bladimiro Rincon-Orozco,[1] Gordana Halec,[2] Simone Rosenberger,[1] Dorothea Muschik,[1] Ingo Nindl,[1] Anastasia Bachmann,[3] Tina Maria Ritter,[1] Bolormaa Dondog,[4] Regina Ly,[1] Franz X. Bosch,[2] Rainer Zawatzky,[1] and Frank Rösl[1]

[1]Angewandte Tumorvirologie, Abteilung Virale Transformationsmechanismen, Deutsches Krebsforschungszentrum, Universität Heidelberg; [2]Molekularbiologisches Labor, Universitäts-HNO-Klinik Heidelberg; [3]Molecular Alcohol Research in Gastroenterology, Universität Heidelberg; and [4]Angewandte Tumorvirologie, Abteilung Genomveränderungen und Karzinogenese, Deutsches Krebsforschungszentrum, Heidelberg, Germany

Abstract

We have investigated interferon-κ (IFN-κ) regulation in the context of human papillomavirus (HPV)–induced carcinogenesis using primary human foreskin keratinocytes (HFK), immortalized HFKs encoding individual oncoproteins of HPV16 (E6, E7, and E6/E7), and cervical carcinoma cells. Here, IFN-κ was suppressed in the presence of E6, whereas its expression was not affected in HFKs or E7-immortalized HFKs. Transcription could be reactivated after DNA demethylation but was decreased again upon drug removal. Partial reactivation could also be accomplished when E6 was knocked down, suggesting a contribution of E6 in IFN-κ *de novo* methylation. We identified a single CpG island near the transcriptional start site as being involved in selective IFN-κ expression. To prove the functional relevance of IFN-κ in building up an antiviral response, IFN-κ was ectopically expressed in cervical carcinoma cells where protection against vesicular stomatitis virus–mediated cytolysis could be achieved. Reconstitution of IFN-κ was accompanied by an increase of p53, MxA, and IFN-regulatory factors, which was reversed by knocking down either IFN-κ or p53 by small interfering RNA. This suggests the existence of a positive feedback loop between IFN-κ, p53, and components of IFN signaling pathway to maintain an antiviral state. Our *in vitro* findings were further corroborated in biopsy samples of cervical cancer patients, in which IFN-κ was also downregulated when compared with normal donor tissue. This is the first report showing an epigenetic silencing of type I IFN after HPV16 oncogene expression and revealing a novel strategy on how high-risk HPVs can abolish the innate immune response in their genuine host cells. [Cancer Res 2009;69(22):8718–25]

Introduction

It is currently well accepted that "high-risk" human papillomaviruses (HPV) are etiologically involved in the development of cervical cancer (1). Although cancer can be induced by various mechanisms, the immune system is a common and indispensable border of defense against the development of malignant tumors. According to the immunosurveillance concept of cancer (2), arising tumors are eradicated by immunologic effector cells or, conversely, immunocompromised individuals should exhibit higher rates of malignancies (3). Indeed, population-based studies show that immunodeficient women have a higher risk to get cervical cancer than age-matched controls (4). This indicates that high-risk HPVs take advantage of a dysfunctional innate and adaptive immunologic surveillance (4–6) to exert their tumorigenic potential.

Considering innate immune evasion strategies, several studies claimed that viral oncoproteins E6 and E7 of high-risk HPVs can potentially target type I interferon (IFN) signal transduction. HPV18 E6 impairs Jak-STAT1/2 tyrosine phosphorylation (7), whereas HPV16 E6 physically interacts with the IFN-regulatory factor (IRF)-3, a central transcription factor in the primary antiviral response (8). However, there is still a matter of controversy because these results do not explain why exogenously added IFN-α or IFN-β induces an antiviral state or why RNA virus infection can activate IRF-3 and, in turn, an immediate-early IFN response in cervical carcinoma cells despite E6 and E7 expression (9, 10).

Although much is known about the function of IFN-α/β in innate and acquired immunity (11, 12), the role of IFN-κ in HPV-mediated pathogenesis is still not defined. IFN-κ shows a very restricted pattern of expression, which is mostly limited to keratinocytes but can be also detected in dendritic cells. IFN-κ strongly binds to heparin, suggesting that it is retained at the local site of production and activates signaling pathways by cell-to-cell contact (13). Because human keratinocytes are the main targets of HPV (1), we have studied the regulation of IFN-κ in the context of HPV-induced carcinogenesis. Evidence is provided that in HPV16 E6-encoding cells, IFN-κ expression is suppressed by *de novo* methylation within a CpG-rich area near the transcriptional start site. Conversely, ectopic expression of IFN-κ in cervical carcinoma cells reconstitutes an antiviral state, which is accompanied by an increase of p53, IRFs, and MxA. Because IFN-κ is the only keratinocyte-specific IFN involved in innate immunity, abrogation of this pathway may represent an early and central key event in the development of cervical cancer.

Materials and Methods

Cell lines and cell treatment. Primary human foreskin keratinocytes (HFK) were immortalized with E6, E7, or E6/E7 oncogenes of HPV16 (14). Normal and HPV-positive HFKs were maintained in keratinocyte growth medium. CaSki, SiHa, HeLa, and C33a cells were cultured as described (15). 5′-Aza-2′-deoxycytidine (5-dAza-C; Calbiochem) was dissolved in 50% acetic acid. Treatment was done using 2.5 to 10 μmol/L as indicated. Sodium butyrate (Sigma) was freshly dissolved in culture medium and trichostatin A (Sigma) was dissolved in DMSO (Merck).

Note: Supplementary data for this article are available at Cancer Research Online (http://cancerres.aacrjournals.org/).

Requests for reprints: Frank Rösl, Angewandte Tumorvirologie, Deutsches Krebsforschungszentrum, Im Neuenheimer Feld 242, 69120 Heidelberg, Germany. Phone: 49-6221-42-4900; Fax: 49-6221-42-4902; E-mail: f.roesl@DKFZ.de.

doi:10.1158/0008-5472.CAN-09-0550

Cell extracts and Western blot analysis. Total cell extracts for Western blot analyses were prepared as reported previously (16). Membranes were probed with the following antibodies: IFN-κ (Abnova); IRF-1, IRF-7, and p53 (Santa Cruz Biotechnology); IRF-9 (Transduction Laboratories); MxA (kindly obtained from Otto Haller, University Freiburg); and actin (ICN Biomedicals).

RNA analysis and real-time PCR. Total RNA from cells or snap-frozen biopsies was isolated using the RNeasy kit (Qiagen). For reverse transcription, 1 μg DNase-treated RNA was prepared as described previously (9). PCR was performed using the 2× green master mix (Promega) according to the manufacturer's instructions. For PCR, the following IFN-κ primers were used: sense 5′-ATGCTTGGAGGAAGACGAGA-3′ and antisense 5′-TTGCGTAGCCACAATCTCTG-3′. Conditions for IFN-κ PCR were as follows: 3 min at 94°C followed by 30 cycles for 30 s at 94°C, 1 min at 58°C, 30 s at 72°C, and 10 min at 72°C. For HPV16, the following primers were used: E6 sense 5′-ACTGCAATGTTTCAGGACCC-3′ and antisense 5′-TCAGGACACAGTGGCTTTTG-3′ and E7 sense 5′-CCCAGCTGTAATCATGCATG-3′ and antisense 5′-TGCCCATTAACAGGTCTTCC-3′. PCR was performed as mentioned above using an annealing temperature of 60°C. Glyceraldehyde-3-phosphate dehydrogenase (GAPDH) primers were sense 5′-TGGATATTGTT - GCCATCAATGACC-3′ and antisense 5′-GATGGCATGGACTGTGGTCATG-3′; amplification was made at 65°C. The PCR products were analyzed on agarose gels.

Quantitative real-time PCR. Quantitative PCR was performed using a TaqMan Universal Master Mix (Applied Biosystems) and TaqMan-specific probes for IFN-κ (Hs00737883-m1) and TATA box binding protein (Hs00427620-m1; Applied Biosystems) according to the manufacturer's instructions. Finally, quantitative PCR was carried out using a real-time PCR (RT-PCR) system (ABI PRISM 7700; Applied Biosystems). The data correspond to the mean from three independent experiments, normalized to TATA box binding protein as reference gene.

McrBC methylation-sensitive PCR. DNA methylation analysis was performed with genomic DNA digested overnight with 10 units McrBC/μg DNA (New England Biolabs; ref. 17). Cleaved DNA was amplified by PCR using 2× green master mix (Promega) with the following IFN-κ primers: region A sense 5′-TTCTAGGATTCAACCTCAAAGC-3′ and antisense 5′-TTCGTCTGGCATAACTGCTG-3′, region B sense 5′-CCATGCCAGGGAAATAAGAA-3′ and antisense 5′-ATGGCTGCACATTTGGCTAT-3′, region C sense 5′-TGCATGGCTGAAAATACAGG-3′ and antisense 5′-TTTTCTGTGGTGAGCAAGTA-3′, region D sense 5′-CAACTGATTGGAACTGAGCC-3′ and antisense 5′-TGGAAGAATAATGGGTGGTTTT-3′, region E sense 5′-GCCATGTTTGTGGAACTGTG-3′ and antisense 5′-TTGACCAAATAACCTTCCTCTGA-3′, and region F sense 5′-TCCTTTTCCCTCGAAATCT-3′ and antisense 5′-TTGCGTAGCCACAATCTCTG-3′. PCR conditions were as follows: 3 min denaturation at 94°C followed for 30 cycles of 30 s at 94°C, 1 min at 58°C, 1 min at 72°C, and 10 min at 72°C.

IFN-κ cloning and transfection of SiHa cells. Human *IFN-κ* gene (Genbank NM_020124) was amplified by PCR with final blunt-end sites using Phusion DNA polymerase (New England Biolabs) and subcloned into the pCMV3tag vector (Stratagene). Human IFN-κ pCMV3tag was transfected using the Fugene-HD reagent (Roche). Selection was done in the presence of 0.5 mg/mL G418 (Invitrogen). G418-resistant colonies were pooled and analyzed.

Antiviral titration assays and Sendai virus infections. Cells were infected with vesicular stomatitis virus (VSV) using multiplicities of infections as described (9). For Sendai virus infection, serum-free medium and Sendai virus (Cantell strain) were added using 32 hemagglutinating units per 4.0×10^5 cells. After 1 h of viral adsorption, the medium was replaced with DMEM containing 10% fetal bovine serum.

Bisulfite sequencing analysis of the IFN-κ promoter. Computer analysis was done using the Methyl Primer Express program (Applied Biosystems). Genomic DNA was isolated using the DNeasy kit (Qiagen) and subjected to bisulfite treatment using the EpiTect Bisulfite kit (Epigentek). DNA was purified and amplified by PCR with the Phusion DNA polymerase (New England Biolabs): One amplified fragment covered a CpG island containing 18 CpG sites localized from positions −2371 to −2115. For amplification, the following primers were used: position −2371 sense 5′-TATTAAATAAGAAATATTTGGTTAGGTATA-3′ and position −2115 antisense 5′-TCACAAATAACTAAAATTACAAACAC-3′. The second amplified fragment covered a stretch of 5 CpG sites located adjacent to the 5′-side of the transcription start site (−276 to −128). For PCR, the following primers were used: position −276 sense 5′-TGTTGGGGATGGATTATTTAGGTATT-3′ and position −128 antisense 5′-TTCAACAAAAAAAATTTTCTCATTC-3′. The amplified fragments were purified using the QIAquick PCR purification kit (Qiagen), cloned into the pJet system (Fermentas), and sequenced.

IFN-κ and p53 small interfering RNA. IFN-κ was targeted with ON-TARGETplus SMART pool L-013217, p53 was targeted with ON-TARGETplus SMART pool L-00332900, and the negative control was targeted with the Nontargeting pool D-001810-10-05 (all obtained from Dharmacon). Small interfering RNA (siRNA) duplexes (40 nmol/L) were transfected into HPV16 E7 HPKs using HiPerFect (Qiagen). Cells were harvested after 72 h (for RNA extraction) and 96 h (for protein extraction) and analyzed as described above.

Immunohistochemical analysis of IFN-κ expression on tissue sections. Tissue sections (4–5 μm) were cut from formalin-fixed, paraffin-embedded biopsies of normal cervical mucosa and cervical carcinoma. Sections were deparaffinized and incubated in 3% H_2O_2 in PBS for 10 min to block endogenous peroxidase. For antigen retrieval, the sections were heated in a pressure cooker in 10 mmol/L citrate buffer (pH 6.0) for 1 min. Nonspecific antibody binding was blocked by incubating with 2.5% normal horse serum. The sections were incubated overnight at 4°C with IFN-κ antibody. For detection, the ImmPRESS peroxidase detection kit was used (Vector Labs). Sections were washed in bi-distilled water, briefly soaked in Meyer's hematoxylin, washed again for 10 min, and dehydrated in ascending ethanol. Xylene was applied twice and the slides were mounted with Eukitt. Consecutive sections to those stained for IFN-κ were stained for the retinoblastoma protein (pRb) and $p16^{INK4a}$ using routinely employed staining protocols as described previously (18).

Results

IFN expression in primary and immortalized human keratinocytes. RT-PCR analyses showed that E7-immortalized cells maintain similar IFN-κ steady-state levels as primary human keratinocytes, whereas IFN-κ was significantly diminished in cells harboring the E6 oncoprotein or in HPV16-positive cervical carcinoma cell lines CaSki and SiHa (Fig. 1*A*). Consistent with the reduction of IFN-κ on the transcriptional level, there was also an absence of the corresponding protein (Fig. 1*B*).

Together with IFN-α/β, IFN-κ belongs to type I IFNs, which transmit their signal through the same receptor complex (19). Similar to IFN-κ (Fig. 1*A*), we showed previously that cervical carcinoma cells also lacked or have reduced IFN-β expression (9, 10). Although it has been reported that HPV16 E7 inhibits TLR9 transcription (20), IFN-β can be alternatively induced through the RIG-1/Mda5–dependent pathway (21) when cells were infected with RNA viruses (22). Because both pattern recognition receptor genes were expressed in our cell systems (Supplementary Fig. S1), we infected cells with Sendai virus known to activate the IRF-3 (22). Figure 1*C* shows that infection strongly induced IFN-β expression in all cells tested. In contrast, IFN-κ transcription could not be activated, suggesting either the lack of specific transcription factors or due to silencing through a *cis*-regulatory mechanism.

Restoration of IFN-κ expression upon demethylation. Considering the latter case, cells were incubated either with inhibitors blocking the activity of histone deacetylases (sodium butyrate or trichostatin A) or with the demethylating agent (5-dAza-C). As depicted in Fig. 2*A*, none of the histone deacetylase inhibitors were able to increase IFN-κ in E6 or E6/E7 cells, indicating that this kind of treatment was not sufficient to reconstitute a functional IFN-κ pathway. Moreover, consistent with previous results (23), type I IFN signaling requires histone deacetylation because the IFN-κ

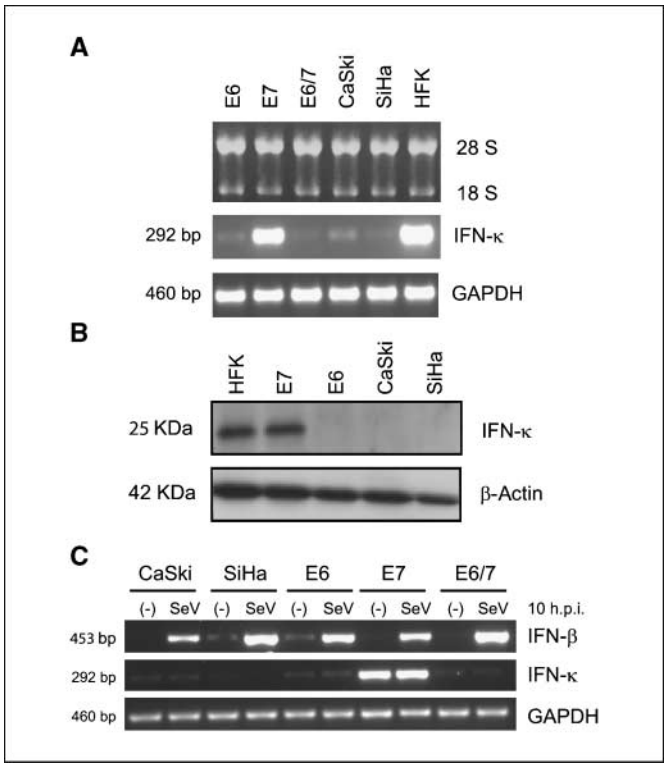

Figure 1. IFN-κ downregulation in HPV16-positive cells. *A,* RT-PCR for IFN-κ and GAPDH in HPV16 E6-, E7-, and E6/E7–immortalized HFKs, CaSki, SiHa, and HFKs. The RT-PCR products were separated on 1.5% agarose gel. The superimposed ethidium bromide gel shows the quality of the RNAs. 18S and 28S: rRNA. *B,* Western blot analysis of IFN-κ. Total cell extracts (100 μg/lane) were separated in a 12% SDS-PAGE. Actin confirms equal loading. *C,* RT-PCR for IFN-β, IFN-κ, and GAPDH in cells 10 h after Sendai virus infection.

steady-state level was even reduced in E7-immortalized keratinocytes in the presence sodium butyrate and trichostatin A. In contrast, treatment with 5-dAza-C resulted in a reactivation of the *IFN-κ* gene in E6- and E6/E7–positive cells (Fig. 2*B, top*), suggesting that the IFN-κ promoter is hypermethylated.

To analyze whether reactivation could also be achieved in cervical carcinoma cell lines, CaSki and SiHa cells were incubated with different concentrations of 5-dAza-C alone or in combination with histone deacetylase inhibitors. Figure 2*B* (*bottom*) shows that 5-dAza-C provoked reexpression of IFN-κ in CaSki cells but not when sodium butyrate was added 24 hours before harvesting. Conversely, no reactivation could be observed in SiHa cells. Decreased stability or inefficient incorporation of the drug cannot account for this because the DNA of both cell lines were demethylated (see Fig. 3*D*). Sequencing the upstream region of IFN-κ failed to show any structural rearrangements or mutations between positions –1964 to –1 relative to the transcriptional start site and corresponds to the Genbank sequence (see NM_020124). Whether there is another mechanism of IFN-κ silencing in SiHa cells remains to be elucidated. IFN-κ could be also induced by 5-dAza-C in HPV18-positive HeLa cervical carcinoma cells, but not in C33a cells, where p53 is found to be mutated (ref. 24; Supplementary Fig. S2*A*).

Nonetheless, there was even a counterselection against 5-dAza-C–mediated IFN-κ reactivation because withdrawal of the drug again resulted in >10-fold reduction of IFN-κ expression as determined by quantitative RT-PCR (Fig. 2*C, bottom*). This indicates that IFN-κ and HPV16 E6 expression seems to be mutually exclusive.

Mapping CpG-rich islands within the IFN-κ regulatory region. Computational analysis of the IFN-κ upstream region (positions –5135 to +1634) revealed two CpG-rich islands located between positions –2371 to –2115 and positions –276 to –128 relative to the transcriptional start site (Fig. 3*A*). To verify their presence *in vivo*, a strategy was applied to scan distinct regions for the presence of methylated DNA (25). Taking advantage of McrBC, a restriction endonuclease that only cleaves DNA when methylated CpG residues are present (17), the appearance of PCR products can be used as indicator for the absence of methylation. The whole upstream region, including parts of the *IFN-κ* gene, was dissected into six fragments (Fig. 3*A*), where PCR products should selectively disappear or be diminished when hypermethylation occurred. Figure 3*B* shows that fragments A, B, C, and F persisted, excluding extensive methylation (see also Supplementary Fig. S2*D*). However, differences became evident when fragments D and E were compared (Fig. 3*C*; Supplementary Fig. S2*D*). Here, region D was cleaved in all cells (*lanes 3, 6,* and *9*, respectively), whereas the fragment covering region E could still be amplified in E7-immortalized keratinocytes (*bottom, lane 3*) but was completely absent in SiHa and CaSki cells (*bottom, lanes 6* and *9*). This indicates that the CpG region was not methylated in E7-immortalized keratinocytes. As shown above (Fig. 2*B*), 5-dAza-C incubation can restore IFN-κ transcription in CaSki but not in SiHa cells. Hence, to perform the reverse experiment, one can predict that demethylated DNA should be protected again from McrBC cleavage when DNA of 5-dAza-C–treated cells is examined. This was indeed the case. Figure 3*C* shows that PCR fragments reappeared and were no longer cleaved by McrBC (*bottom*, compare *lanes 5* and *6* as well as *lanes 8* and *9*).

Fine analysis after the bisulfite sequencing (26) indicated that the methylation pattern within region D (positions –2371 to –2115) was almost identical (Fig. 3*D, left*). In contrast, all cells lacking IFN-κ expression revealed strong hypermethylation within region E, whereas the corresponding DNA was almost methylation-free in primary and E7-positive keratinocytes. Moreover, bisulfite sequencing after 5-dAza-C treatment (Fig. 3*D, right*) also showed that despite differences in IFN-κ reactivation in SiHa and CaSki cells, DNA became demethylated in both cell lines.

Reconstitution of IFN-κ restores antiviral activity. Because our previous studies have shown that cervical carcinoma cells are extremely sensitive to infection with VSV due to their lack of type I IFN expression (9, 10), we next tested whether reconstitution of IFN-κ can protect malignant HPV16-positive cells against viral infection. For this purpose, the cDNA of IFN-κ was stably introduced in SiHa cells along with a dominant selection marker. To avoid position effects of integrated DNA in individual clones, G418-resistant cells were pooled and analyzed. Although restored IFN-κ expression was not affecting the steady-state level of viral E6/E7 transcription (Fig. 4*A*), the p53 protein level was enhanced. Moreover, IFN-κ–positive SiHa cells also showed a significant increase of IRF-1, IRF-7, and IRF-9, all key regulatory proteins involved in immediate and delayed IFN response (27). Concomitantly to p53 and IRFs, MxA as a central component of an IFN-induced antiviral state (28) was also found to be upregulated (Fig. 4*B*).

To examine whether the IFN-κ–specific mRNA was translated into functional protein to build up an antiviral response, protection assays against VSV-mediated cytolysis were carried out (Fig. 4*C*). VSV is a member of the Rhabdoviridae RNA virus family, being exceptionally sensitive to type I IFN (29). As already

seen after staining (Fig. 4*C, top*), quantification reveals that IFN-κ–positive SiHa cells were strongly protected against VSV infection (*bottom*), clearly showing that reconstituted IFN-κ leads to an antiviral state.

Because enhanced p53 levels can improve the type I IFN response (30) and vice versa (31), we next asked whether knocking down constitutive IFN-κ expression in E7-positive keratinocytes had a reverse effect. As shown in Fig. 4*D* (*top*), siRNA directed against IFN-κ significantly reduced p53, IRF-1, IRF-7, IRF-9, and MxA, strongly supporting the notion that constitutive IFN-κ expression maintains threshold levels of p53, which, in turn, guarantees to conserve an alert antiviral state. A positive regulatory circuit between IFN-κ and p53, as well as type I IFN downstream targets, could also be shown when p53 was knocked down after siRNA delivery (Fig. 4*D, bottom*).

IFN-κ is not expressed in cervical cancer biopsies. To estimate the clinical relevance of our *in vitro* data, RNAs from tumor samples and normal biopsies were monitored by RT-PCR for the presence of HPV16 E6 and IFN-κ. Figure 5*A* illustrates that, in contrast to HPV16-negative control tissues, cervical cancer samples showed impaired IFN-κ expression, inversely correlating with viral transcription. Immunohistochemical examination of tissue specimen from patients positive for HPV16 lacked IFN-κ staining in all cervical tumor sections examined thus far (10 of 10). Figure 5*B* to *D* depicts a representative example of a HPV16-positive cervical tumor section, where the overview showed histologically normal squamous epithelium as well as features of a grade 1 cervical intraepithelial neoplasia (CIN1). As shown in histologically normal mucosal areas, most of the cells in parabasal and suprabasal layers were positive for IFN-κ, whereas there was weaker staining in CIN1, which was absent in the corresponding tumor region. Control staining for the pRb (Fig. 5*C*) illustrates decreased pRb with increasing progression of the lesions. Conversely, there was a strong increase of $p16^{INK4a}$ (Fig. 5*D*), known to be negatively regulated by pRb (32). In conclusion, these data indicate that the loss of IFN-κ expression is an early event in HPV-induced carcinogenesis, the absence of which could be considered as an additional marker for progressing lesions.

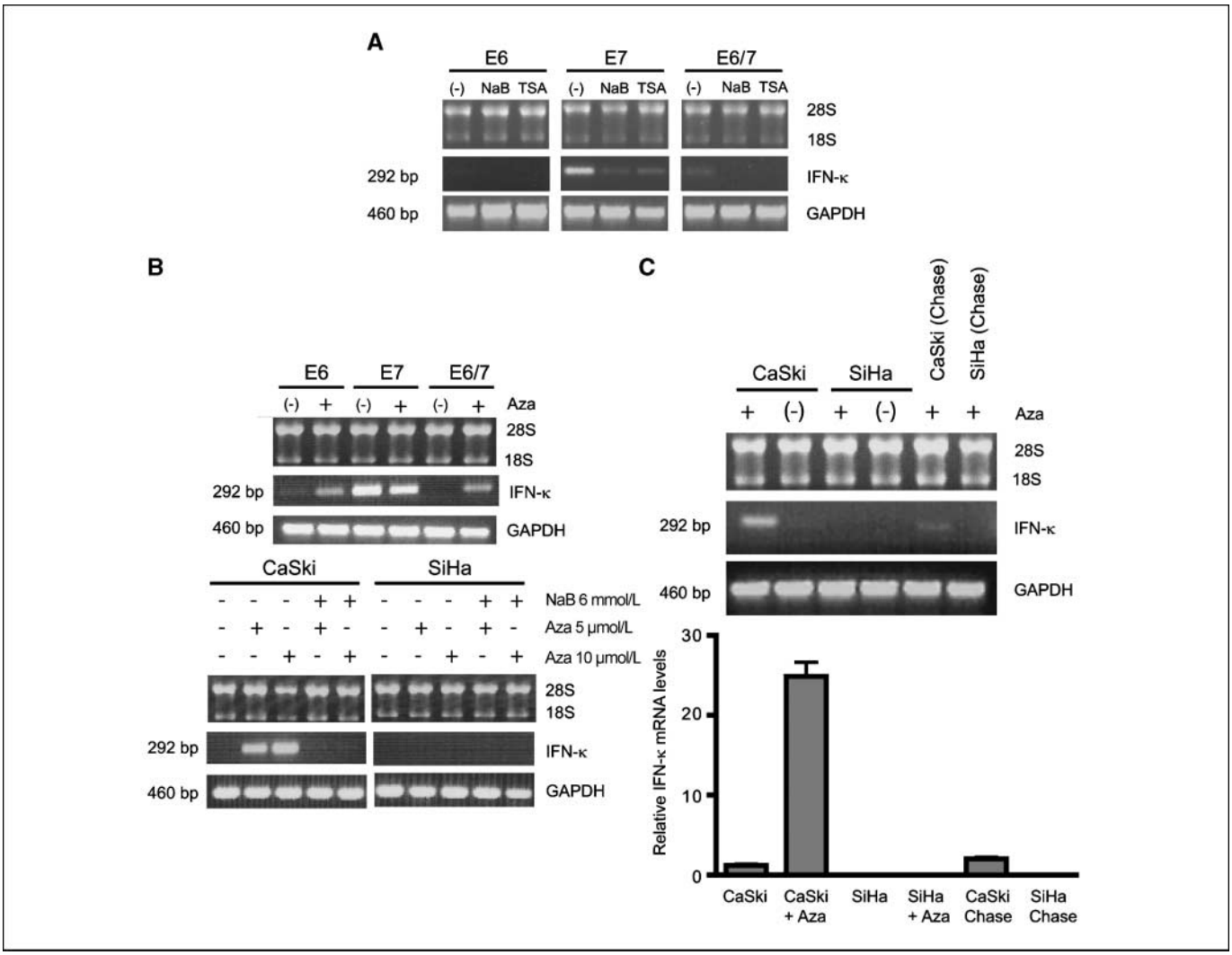

Figure 2. Reactivation of IFN-κ transcription after DNA demethylation. *A,* RT-PCR for IFN-κ and GAPDH in cells treated with sodium butyrate (*NaB*; 6 mmol/L) or trichostatin A (*TSA*; 330 nmol/L) for 24 h. *B, top,* RT-PCR for IFN-κ and GAPDH in cells treated with 5-dAza-C (*Aza*; 2.5 μmol/L) for 96 h; *bottom,* RT-PCR analysis for IFN-κ and GAPDH in cells treated with different concentrations of 5-dAza-C (5-10 μmol/L) for 96 h and sodium butyrate for 24 h. *C, top,* RT-PCR analysis for IFN-κ and GAPDH in cells treated with 5-dAza-C (10 μmol/L) for 96 h and/or after subsequent cultivation in normal medium for an additional 96 h (*Chase*). *Bottom,* quantitative PCR analysis of IFN-κ mRNA levels. The ordinate represents the relative IFN-κ levels normalized against TATA box binding protein as reference gene.

Discussion

Our data show that primary human keratinoyctes, as well as immortalized cells only encoding the HPV16 E7 oncoprotein, maintain constitutive IFN-κ expression, whereas the gene is strongly suppressed in E6- and E6/E7–positive cells as well as in HPV16/18 cervical carcinoma cell lines (Fig. 1*A*; see Supplementary Fig. S2). Notably, IFN-κ expression already becomes downregulated during initial immortalization *in vitro* even in the absence of any immunomodulatory environment. IFN-κ reduction occurred 2 weeks after HPV16 E6 delivery through amphotropic retroviruses (Supplementary Fig. S2*B*), supporting the idea that IFN-κ dysregulation can be considered as an early event in virus-induced

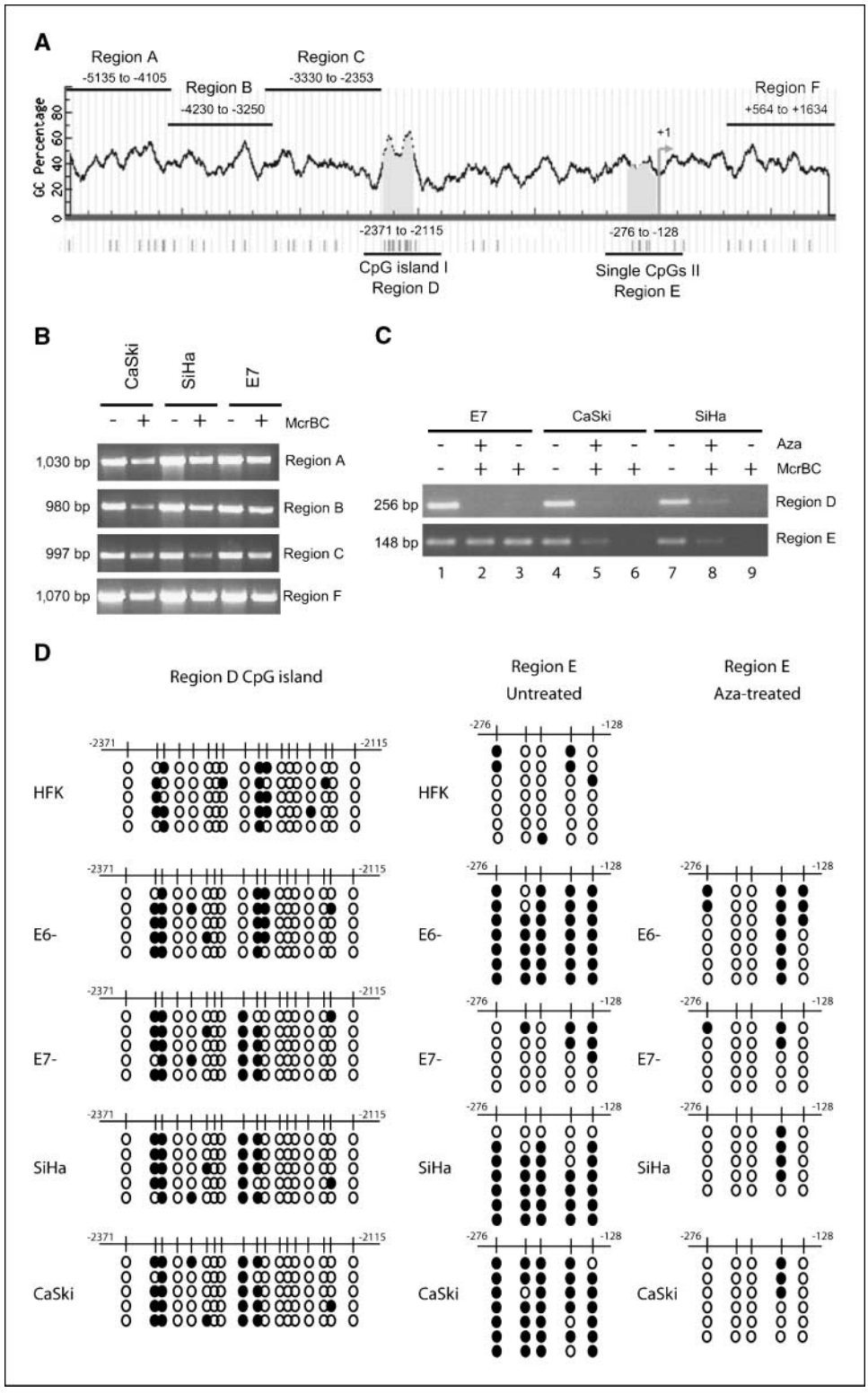

Figure 3. *De novo* methylation within the IFN-κ promoter. *A,* schematic presentation of the IFN-κ promoter and 5′-end of the gene showing the location of CpG sequences (*thin vertical line*) and CpG islands. The transcriptional start site is indicated as +1 and CpG islands are indicated as a gray shatter. The ordinate represents the percentage of CpG. *B,* McrBC cleavage and subsequent PCR using different primers covering regions A, B, C, and F (see above). *C,* same as in *B*, analyzing regions D and E. *D,* bisulfite sequencing of regions D (*left*) and E (*right*) of the cells. Each horizontal set of circles represents the methylation pattern of a single sequenced PCR product. ●, methylation; ○, unmethylated CpGs. The methylation pattern of untreated and 5-dAza-C–treated DNA is also shown.

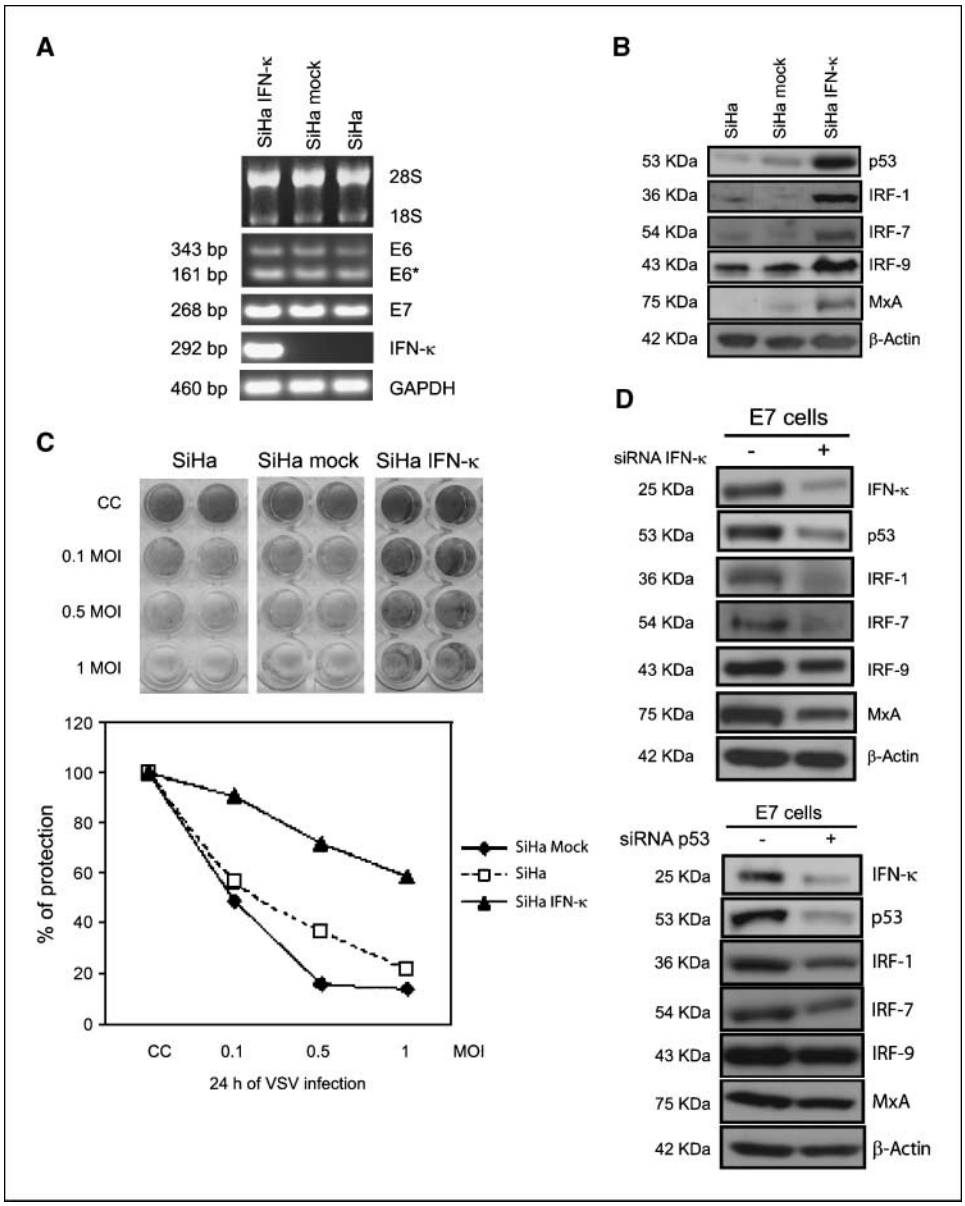

Figure 4. Ectopic expression/siRNA knockdown of IFN-κ and p53. *A,* RT-PCR for IFN-κ and E6/E7 expression in transfected and mock-transfected SiHa cells. *B,* Western blot analysis for p53, IRF-1, IRF-7, IRF-9, and MxA using 100 μg/lane of total cell extract. *C, top,* selective protection against infection using VSV at different multiplicities of infections (*MOI*) as indicated (*CC,* uninfected control). *SiHa Mock,* empty vector transfection; *SiHa IFN-κ,* IFN-κ–transfected cells. *Bottom,* percentage of cells killed after infection. All SDs (range between 1.93 and 3.4) are given for five independent experiments performed in triplicate. *D, top,* E7-immortalized keratinocytes were transfected with siRNAs against IFN-κ or with scrambled siRNA as control and Western blot analysis was performed. *Bottom,* same as the top panel but using siRNA against p53.

carcinogenesis. This is further substantiated by the finding that IFN-κ is also diminished in precursor lesions and finally absent in cervical cancer samples (Fig. 5).

The development of cancer can be regarded as an evolutionary process (33), in which genes that are not compatible with cell proliferation are turned off either by irreversible genetic loss or by reversible downregulation through epigenetic means (34). Moreover, there even exists a cross-talk between *cis*- and *trans*-regulatory mechanisms because decreased transcriptional activity due to the presence/absence of a putative *trans*-repressor/activator can trigger epigenetic alterations (35, 36). Such a situation marks promoter sequences for histone modifications and *de novo* methylation, finally leading to suppression of the respective gene (37–39).

HPV16/18 apparently act through both of these mechanisms. As shown previously, cervical carcinoma cells lack the ability to express IFN-β on TNF-α treatment, which was mainly attributed to the absence of the IRF-1, an important *trans*-acting activator of the IFN-β promoter (9, 10). However, IFN-β as intermediate-early IFN (40) can be reactivated after infection with RNA viruses (21, 22), where IRF-3 is replacing IRF-1 in building up the IFN-β enhanceosome (41). This efficiently operates for IFN-β but not for IFN-κ (Fig. 1*C*), which we considered as experimental hint that the gene might be locked by a *cis*-regulatory mechanism (Figs. 2 and 3). In fact, as revealed by PCR-based "bisulfite sequencing" (42), there is a 148-bp DNA sequence (positions −276 to −128) close to the transcriptional start site that is hypermethylated in E6- and E6/E7–immortalized HFKs as well as in cervical carcinoma cells but not in E7-expressing cells or primary HFKs (Fig. 3*D*). IFN-κ transcription, however, could be reconstituted when the cells were treated with 5-dAza-C (Fig. 2*B*). Apparently, there is even a counterselection against functional reactivation of IFN-κ because withdrawal of 5-dAza-C again reduced expression (Fig. 2*C*). Hence, continuous expression of HPV16 E6 seems to be necessary to maintain IFN-κ suppression because siRNA directed against E6 lead to a reactivation of IFN-κ after 72 hours (Supplementary Fig. S2*C*).

In contrast, no reactivation could be achieved when cells were treated with inhibitors of histone deacetylases (Fig. 2*A* and *B*). Although histone deacetylases are known to act as corepressors instead of coactivators in modulating gene expression, their function as positive regulators of IFN signaling is well established (23, 43, 44).

Transcriptional silencing of proinflammatory cytokines by hypermethylation is not without precedence. Considering IFN-γ for instance, there is differential cytokine expression in naive versus memory CD8 T cells, which is controlled by epigenetic mechanisms. Whereas the hypermethylated *IFN-γ* gene is only induced after longer incubation with 5-dAza-C in naive T-cells, the regulatory region of IFN-γ in memory cells is demethylated within hours after antigen exposure (45). Referring to our system, continued demethylation is necessary for transcription, suggesting that activation of IFN-κ required cell division and chromatin remodeling before the gene could be transcribed (46). Although E7 of HPV16 can interact with and activate DNA methyltransferase Dnmt1 (47), this kind of interaction cannot account for gene silencing because IFN-κ transcription is not biased in E7-positive cells (Fig. 1*A*).

Of note is the finding that reexpression of IFN-κ in SiHa cells (Fig. 4*A*) leads to an induction of an antiviral state by upregulation of p53, IRFs, and MxA (Fig. 4*B*), resulting in a protective effect against VSV infection (Fig. 4*C*). Here, p53 is increased without changes in the viral splicing pattern of E6 in favor to E6*, known to counteract p53 degradation (48). This supports the previous finding of a functional cross-talk between type I IFN signal transduction and p53 upregulation (49). Consequently, increased levels of p53, in turn, seem to enhance the IFN response in a way that an antiviral alert is induced (30). Considering this scenario in terms of the ectopic reconstitution of IFN-κ in SiHa cells (Fig. 4*A*) and the siRNA knockdown experiments of IFN-κ and p53 in E7-expressing HFKs (Fig. 4*D*), the following model can be envisioned: high-risk HPV E6 expression leads to both p53 degradation (48) and *de novo* methylation of IFN-κ in the host cells (Fig. 3). This interferes with an apparent cross-talk between IFN-κ and p53 (and vice versa), which consecutively affects the expression of IRF-1, IRF-7, IRF-9, and MxA (Fig. 4), all known to be p53-responsive genes (30). p53 can be also induced by type I IFN through IFN-stimulated response element–like sequences within the promoter and the first intron regions (19), which may, in turn, activate constitutive IFN-κ

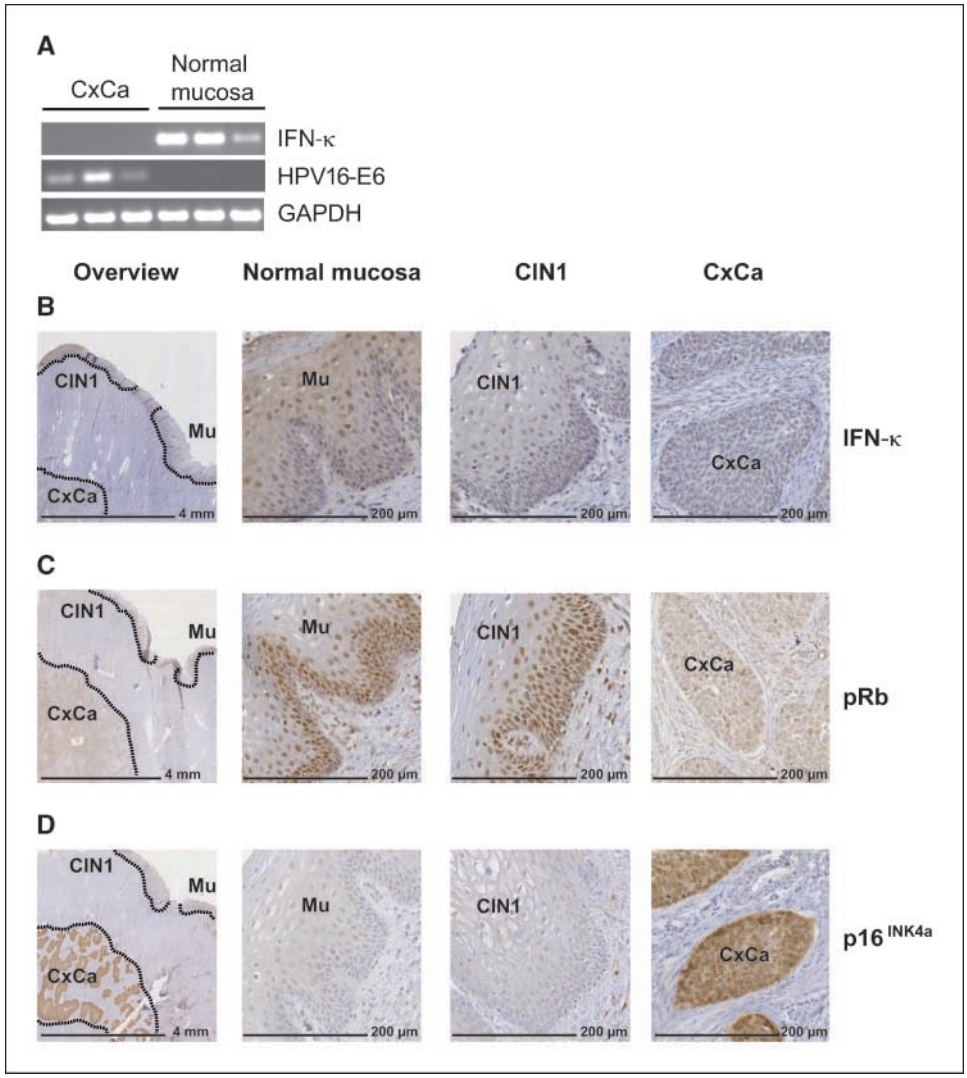

Figure 5. IFN-κ expression in normal and HPV16-positive cervical tissues. *A,* RT-PCR for IFN-κ, HPV16 E6, and GAPDH from cervical cancer (*CxCa*) and normal mucosa (*Mu*). *B,* IFN-κ staining overview of the section. *Bar,* 4 mm. Normal area with IFN-κ positivity. Diminished positive staining in precancerous lesions (CIN1). Negative IFN-κ staining in cervical cancer. *Bar,* 200 μm. *C,* pRb staining, overview of the section. Normal mucosa with pRb positivity. Positive staining in CIN1. Cervical cancer: low pRb expression. *D,* $p16^{INK4a}$ staining, overview of the section. Normal mucosa with negative stain. Very low positivity for $p16^{INK4a}$ in CIN1. Tumor area with high $p16^{INK4a}$ expression.

expression by a positive regulatory circuit (Fig. 4*B* and *D*). Although only reported up to now in rodent cells, constitutive activation of type I IFN can prevent cellular transformation (50), which may be also true for human keratinocytes (Fig. 1*A*). An explanation of how E6 is mediating IFN-κ silencing could be through downregulation of IRF7 (Fig. 4*D*), which has a potential *in silico* binding site within the proximal CpG island (positions −118 to −98), targeted by *de novo* methylation (Fig. 3*D*). Reduced transcriptional activity as a consequence of IRF-7 reduction could mark this region for epigenetic modification, which is otherwise counterbalanced by constitutive IFN-κ expression through the above-mentioned positive regulatory loop.

The situation deduced from cell culture studies seem to be valid also for the *in vivo* situation. Downregulation of IFN-κ was evident already in tumor-adjacent cervical mucosa displaying CIN1 morphology (Fig. 5), which is in analogy to immortalized keratinocytes grown under *in vitro* conditions (Fig. 1).

In conclusion, these data identify the *IFN-κ* gene as a novel target of high-risk HPVs, where the genuine host innate immune response becomes suppressed by an epigenetic mechanism.

Disclosure of Potential Conflicts of Interest

No potential conflicts of interest were disclosed.

Acknowledgments

Received 2/17/09; revised 9/2/09; accepted 9/14/09; published OnlineFirst 11/3/09.

The costs of publication of this article were defrayed in part by the payment of page charges. This article must therefore be hereby marked *advertisement* in accordance with 18 U.S.C. Section 1734 solely to indicate this fact.

We thank Denise Galloway (Fred Hutchinson Center) for providing the amphotropic retroviral constructs and the producer cell lines, Richard Schlegel (Department of Pathology, Georgetown University Medical School) for the HPV16 E6/E7 immortalized human keratinocytes, and Felix Hoppe-Seyler (German Cancer Research Center) for the siRNAs against HPV16/18 E6 oncoprotein.

References

1. zur Hausen H. Papillomaviruses and cancer: from basic studies to clinical application. Nat Rev Cancer 2002;2:342–50.
2. Stagg J, Johnstone RW, Smyth MJ. From cancer immunosurveillance to cancer immunotherapy. Immunol Rev 2007;220:82–101.
3. Dunn GP, Bruce AT, Ikeda H, Old LJ, Schreiber RD. Cancer immunoediting: from immunosurveillance to tumor escape. Nat Immunol 2002;3:991–8.
4. Tindle RW. Immune evasion in human papillomavirus-associated cervical cancer. Nat Rev Cancer 2002;2:59–65.
5. Lambris JD, Ricklin D, Geisbrecht BV. Complement evasion by human pathogens. Nat Rev Microbiol 2008; 6:132–42.
6. Kanodia S, Fahey LM, Kast WM. Mechanisms used by human papillomaviruses to escape the host immune response. Curr Cancer Drug Targets 2007;7:79–89.
7. Li S, Labrecque S, Gauzzi MC, et al. The human papilloma virus (HPV)-18 E6 oncoprotein physically associates with Tyk2 and impairs Jak-STAT activation by interferon-α. Oncogene 1999;18:5727–37.
8. Ronco LV, Karpova AY, Vidal M, Howley PM. Human papillomavirus 16 E6 oncoprotein binds to interferon regulatory factor-3 and inhibits its transcriptional activity. Genes Dev 1998;12:2061–72.
9. Bachmann A, Hanke B, Zawatzky R, et al. Disturbance of tumor necrosis factor α-mediated β interferon signaling in cervical carcinoma cells. J Virol 2002;76:280–91.
10. Bachmann A, Zawatzky R, Rosl F. Genetic redundancy in human cervical carcinoma cells: identification of cells with "normal" properties. Int J Cancer 2007;120:2119–26.
11. Noppert SJ, Fitzgerald KA, Hertzog PJ. The role of type I interferons in TLR responses. Immunol Cell Biol 2007;85:446–57.
12. Alsharifi M, Mullbacher A, Regner M. Interferon type I responses in primary and secondary infections. Immunol Cell Biol 2008;86:239–45.
13. Buontempo PJ, Jubin RG, Buontempo CA, Wagner NE, Reyes GR, Baroudy BM. Antiviral activity of transiently expressed IFN-κ is cell-associated. J Interferon Cytokine Res 2006;26:40–52.
14. Aguilar-Lemarroy A, Gariglio P, Whitaker NJ, et al. Restoration of p53 expression sensitizes human papillomavirus type 16 immortalized human keratinocytes to CD95-mediated apoptosis. Oncogene 2002;21:165–75.
15. Soto U, Denk C, Finzer P, Hutter KJ, zur Hausen H, Rosl F. Genetic complementation to non-tumorigenicity in cervical-carcinoma cells correlates with alterations in AP-1 composition. Int J Cancer 2000;86:811–7.
16. Soto U, Das BC, Lengert M, Finzer P, zur Hausen H, Rosl F. Conversion of HPV 18 positive non-tumorigenic HeLa-fibroblast hybrids to invasive growth involves loss of TNF-α mediated repression of viral transcription and modification of the AP-1 transcription complex. Oncogene 1999;18:3187–98.
17. Sutherland E, Coe L, Raleigh EA. McrBC: a multisubunit GTP-dependent restriction endonuclease. J Mol Biol 1992;225:327–48.
18. Karsai S, Abel U, Roesch-Ely M, et al. Comparison of p16 (INK4a) expression with p53 alterations in head and neck cancer by tissue microarray analysis. J Pathol 2007;211:314–22.
19. Takaoka A, Yanai H. Interferon signalling network in innate defence. Cell Microbiol 2006;8:907–22.
20. Hasan UA, Bates E, Takeshita F, et al. TLR9 expression and function is abolished by the cervical cancer-associated human papillomavirus type 16. J Immunol 2007;178:3186–97.
21. Takeuchi O, Akira S. MDA5/RIG-I and virus recognition. Curr Opin Immunol 2008;20:17–22.
22. Bose S, Banerjee AK. Innate immune response against nonsegmented negative strand RNA viruses. J Interferon Cytokine Res 2003;23:401–12.
23. Nusinzon I, Horvath CM. Positive and negative regulation of the innate antiviral response and β interferon gene expression by deacetylation. Mol Cell Biol 2006;26:3106–13.
24. Scheffner M, Munger K, Byrne JC, Howley PM. The state of the p53 and retinoblastoma genes in human cervical carcinoma cell lines. Proc Natl Acad Sci U S A 1991;88:5523–7.
25. Badal S, Badal V, Calleja-Macias IE, et al. The human papillomavirus-18 genome is efficiently targeted by cellular DNA methylation. Virology 2004;324:483–92.
26. Olek A, Oswald J, Walter J. A modified and improved method for bisulphite based cytosine methylation analysis. Nucleic Acids Res 1996;24:5064–6.
27. Tamura T, Yanai H, Savitsky D, Taniguchi T. The IRF family transcription factors in immunity and oncogenesis. Annu Rev Immunol 2008;26:535–84.
28. Haller O, Stertz S, Kochs G. The Mx GTPase family of interferon-induced antiviral proteins. Microbes Infect 2007;9:1636–43.
29. Meager A. Biological assays for interferons. J Immunol Methods 2002;261:21–36.
30. Munoz-Fontela C, Macip S, Martinez-Sobrido L, et al. Transcriptional role of p53 in interferon-mediated antiviral immunity. J Exp Med 2008;205:1929–38.
31. Taniguchi T, Takaoka A. A weak signal for strong responses: interferon-α/β revisited. Nat Rev Mol Cell Biol 2001;2:378–86.
32. Nakao Y, Yang X, Yokoyama M, et al. Induction of p16 during immortalization by HPV 16 and 18 and not during malignant transformation. Br J Cancer 1997;75:1410–6.
33. Merlo LM, Pepper JW, Reid BJ, Maley CC. Cancer as an evolutionary and ecological process. Nat Rev Cancer 2006;6:924–35.
34. Feinberg AP. Phenotypic plasticity and the epigenetics of human disease. Nature 2007;447:433–40.
35. Fuks F. DNA methylation and histone modifications: teaming up to silence genes. Curr Opin Genet Dev 2005; 15:490–5.
36. Wade PA. SWItching off methylated DNA. Nat Genet 2005;37:212–3.
37. Mutskov V, Felsenfeld G. Silencing of transgene transcription precedes methylation of promoter DNA and histone H3 lysine 9. EMBO J 2004;23:138–49.
38. Stirzaker C, Song JZ, Davidson B, Clark SJ. Transcriptional gene silencing promotes DNA hypermethylation through a sequential change in chromatin modifications in cancer cells. Cancer Res 2004;64:3871–7.
39. De-Castro Arce J, Gockel-Krzikalla E, Rosl F. Retinoic acid receptor β silences human papillomavirus-18 oncogene expression by induction of *de novo* methylation and heterochromatinization of the viral control region. J Biol Chem 2007;282:28520–9.
40. Honda K, Takaoka A, Taniguchi T. Type I interferon [corrected] gene induction by the interferon regulatory factor family of transcription factors. Immunity 2006;25:349–60.
41. Yoneyama M, Suhara W, Fukuhara Y, Fukuda M, Nishida E, Fujita T. Direct triggering of the type I interferon system by virus infection: activation of a transcription factor complex containing IRF-3 and CBP/p300. EMBO J 1998;17:1087–95.
42. Frommer M, McDonald LE, Millar DS, et al. A genomic sequencing protocol that yields a positive display of 5-methylcytosine residues in individual DNA strands. Proc Natl Acad Sci U S A 1992;89:1827–31.
43. Chen J, Baig E, Fish EN. Diversity and relatedness among the type I interferons. J Interferon Cytokine Res 2004;24:687–98.
44. Chang HM, Paulson M, Holko M, et al. Induction of interferon-stimulated gene expression and antiviral responses require protein deacetylase activity. Proc Natl Acad Sci U S A 2004;101:9578–83.
45. Kersh EN, Fitzpatrick DR, Murali-Krishna K, et al. Rapid demethylation of the IFN-γ gene occurs in memory but not naive CD8 T cells. J Immunol 2006;176:4083–93.
46. Fahrner JA, Baylin SB. Heterochromatin: stable and unstable invasions at home and abroad. Genes Dev 2003;17:1805–12.
47. Burgers WA, Blanchon L, Pradhan S, de Launoit Y, Kouzarides T, Fuks F. Viral oncoproteins target the DNA methyltransferases. Oncogene 2007;26:1650–5.
48. Pim D, Massimi P, Banks L. Alternatively spliced HPV-18 E6* protein inhibits E6 mediated degradation of p53 and suppresses transformed cell growth. Oncogene 1997;15:257–64.
49. Takaoka A, Hayakawa S, Yanai H, et al. Integration of interferon-α/β signalling to p53 responses in tumour suppression and antiviral defence. Nature 2003;424:516–23.
50. Chen HM, Tanaka N, Mitani Y, et al. Critical role for constitutive type I interferon signaling in the prevention of cellular transformation. Cancer Sci 2009;100:449–56.